SIMULATION OF A REFILL FRICTION STIR SPOT WELDING PROCESS

Dan BIRSAN[1]

[1] *"Dunarea de Jos" University of Galati, dbirsan@ugal.ro.*

Abstract: *Friction spot joining technology (FSSW) takes place in the solid state, which makes the residual stresses after welding has lower values than in the case of fusion welding. For this reason, this joining technology can replace processes such as resistance spot welding and rivet technology in certain applications. The complex physical phenomena that occur during the welding process such as frictional contact, high-temperature gradients, and large dimensions make it necessary to know the process parameters in detail for their optimization.*

This work developed a finite element model containing two aluminum plates welded by the refill friction stir spot welding process, the simulation results include temperature, strain, and stress distributions. The simulation results were compared with the data available in the specialized literature and validated.

Keywords: *friction, welding, finite element, stress, temperature*

1. Introduction

This work developed a finite element model containing two aluminum plates welded by the refill friction stir spot welding process, the simulation results include temperature, strain, and stress distributions.

Aluminum alloy 5083-O is considered for automotive and marine applications due to its low density and yield stress comparable to some steels.

Frictional refill spot welding (FSSW refill) is a solid state joining process that allows two or more sheets to be joined in an overlapping configuration.

This process allows making welds without solidification defects. FSSW filler has been successfully applied to join dissimilar and dissimilar metals and recently, Barros and co. Ref. [7] reported the joining of aluminum alloy AA2198. Kubit et al. Ref. [1] modeled and validated refill friction stir spot welding of Alclad 7075-T6 aluminum alloy sheets.

Zou and co. Ref. [2] presents the formability and mechanical property of refill friction stir spot–welded joints and some conclusions of this work are: the increase of rotation speed has no apparent influence on the hook defect morphology of the joints (with increasing the plunge depth, the height of the hook defect increases), the higher tensile-shear strength is associated with increased rotation speed.

Friction stir spot welding of aluminum alloy 6061-T6 sheets, experimental and simulation analysis has been performed by D'Urso and co. Ref. [3] using the commercial FEM code Deform 3D.

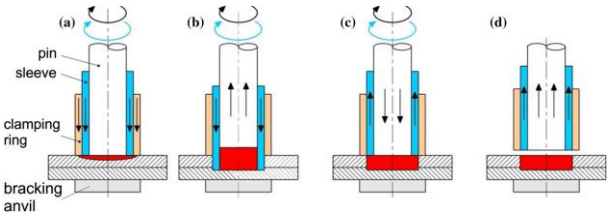

Figure 1: *Stages of the RFSSW process: touchdown and preheating (a), plunging (b), refilling (c), and retreating (d)*[1]

2. Constitutive Laws

For the viscoplastic material, the flow stress $(\bar{\sigma})$, is commonly defined as a function of equivalent plastic strain-rate tensor ($\dot{\varepsilon}_{eq}$) and the temperature (T) (Ref. [12]):

$$\bar{\sigma} = f(\dot{\varepsilon}_{eq}, T), \dot{\varepsilon}_{eq} < 1000[s^{-1}] \quad (1)$$

where $\dot{\varepsilon}_{eq}$ was calculated with formulae:

$$\dot{\varepsilon}_{eq}^2 = \frac{2}{3}\dot{\varepsilon}_{ij}\dot{\varepsilon}_{ij} \quad (2)$$

According to Ref. [12] a constitutive law for the viscoplastic materials, as a function of the equivalent strain-rate and flow stress can be written as:

$$\mu = \frac{\bar{\sigma}(\dot{\varepsilon}_{eq}, T)}{2\dot{\varepsilon}_{eq}} \quad (3)$$

Sheppard and Wright (Ref. 13) introduced the flow stress $\bar{\sigma}$ for the large and high strain-rate bulk deformation processes of metals as following:

$$\bar{\sigma} = \frac{1}{\alpha} sinh^{-1}\left(\left(\frac{Z}{A}\right)^{1/n}\right) \quad (4)$$

where $Z = \dot{\varepsilon}_{eq} \cdot \exp\left(\frac{Q}{RT}\right)$.

3. Finite-element modeling

The numerical model developed allows a detailed analysis of the phenomena that occur during the formation of the weld and of the relationships that occur at the interface between the tool surface and the sheets. After the analysis with finite elements, the obtained results must be in accordance with the experimental ones in order to be validated.

The validation of the analysis with finite elements can also come by comparing the results obtained with those found in the specialized literature.

Numerical analysis of the RFSSW process has been performed using Simufact Forming software (Simufact Engineering Gmbh, Hamburg, Germany). The coupled thermo-mechanical analysis has been performed to obtain the distribution of temperature, the deformations and the stresses of the material during the welding process.

Table 1: *Chemical composition of AA5083-O*

Al	Mg	Si	Fe	Cu	Cr	Zn	Ti	Mn
92.4	4.0	0.0	0.0	0.0	0.05	0.0	0.0	0.4
95.6	4.9	0.4	0.4	0.1	0.25	0.25	0.1	1.0

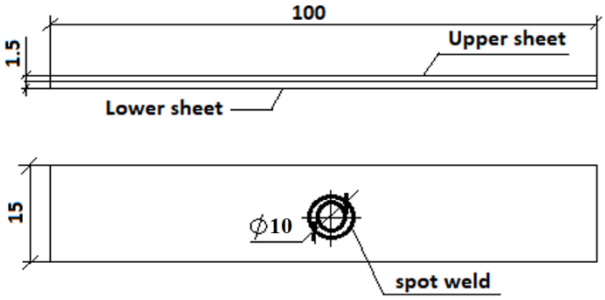

Figure 1: *Dimensions (in mm) of the welding specimens*

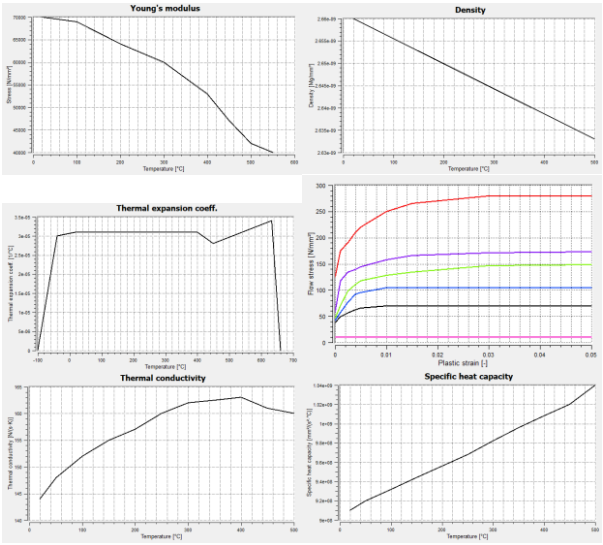

Figure 2: *AA 5083-O thermal and mechanical properties*

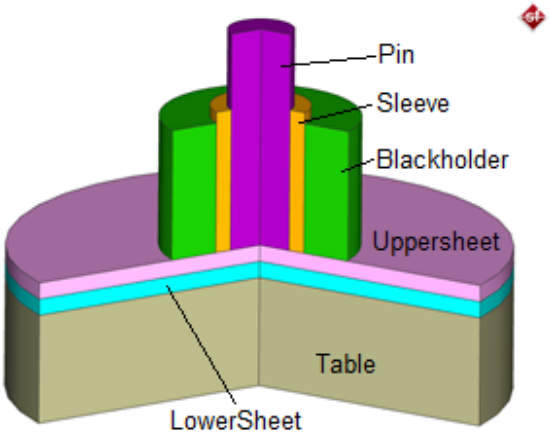

Figure 3: *Finite-element model*

The boundary conditions were adopted to take into account the influence of external factors on the model, avoiding possible unrealistic demands that may appear in the areas of interest.

The following welding parameters have been used in experiments: clamping force 15kN, tool rotational speed 2000rpm, and tool plunge depth 1.4mm. The welding cycle consists of plunge time (1 s) and tool retracts time (1 s).

The welding tool used consists of three independent elements (Fig. 3): 20mm diameter clamping ring, 10mm diameter of sleeve and 5.5mm diameter of pin.

4. Results and Discussions

4.1. Temperature field distribution

In Fig. 4 and 5 show the thermal fields during the welding process in two moments of time, the first is at 1s, at the end of the advance of the sleeve and the second at the end of the welding moment.

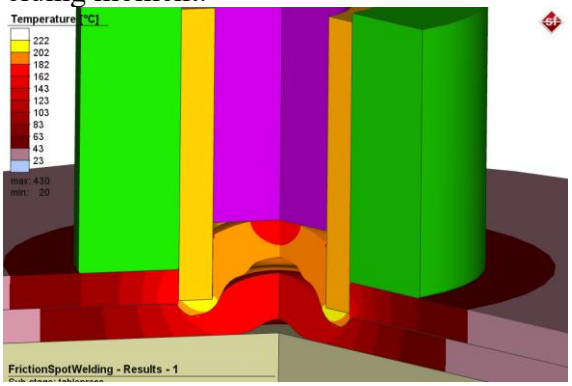

Figure 4: *Thermal field at 1s*

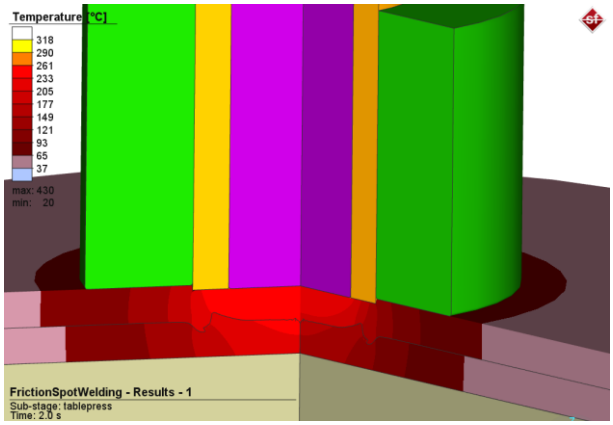

Figure 5: *Thermal field at the end of the welding process*

The maximum temperature time variations of in the upper and lower plates are shown in Fig. 6. The maximum temperature reached during the welding process in the upper plate is 420°C and in the lower plate 225°C.

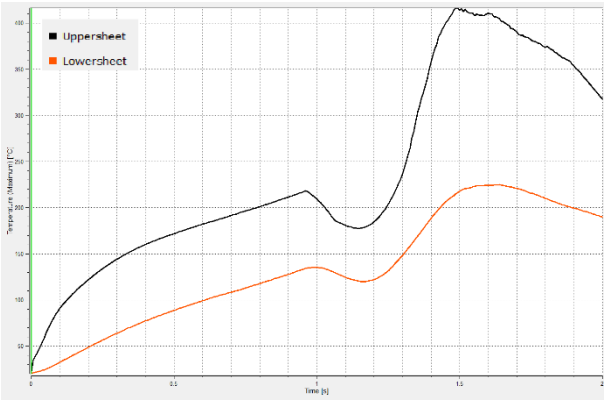

Figure 6: *Thermal history plot of the upper and lower plates*

4.2. Von Mises stresses and plastic strain

The effective stresses that appear during the welding process are directly proportional to the degree of deformation of the parts and inversely proportional to the temperature reached in them. In Figs. 7 and 8 the effective stresses in the welded joint can be observed in two moments of time, during and at the end of the welding process. The effective stress of a welded joint depends on its temperature. It can be seen that the maximum stress occurs in the most deformed area, the maximum reaching 323N/mm^2. The residual stresses in the plates are 279N/mm^2.

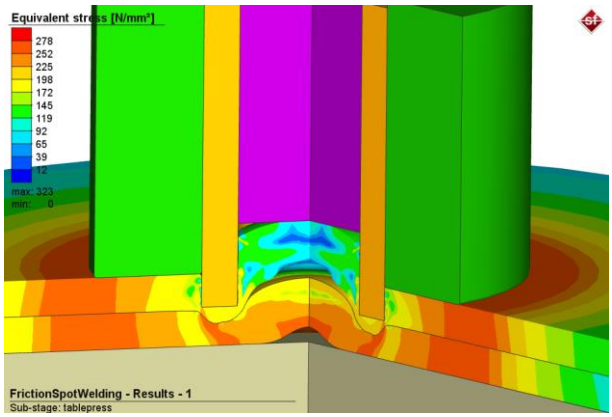

Figure 7: *Effective stresses distribution in plates at 1s*

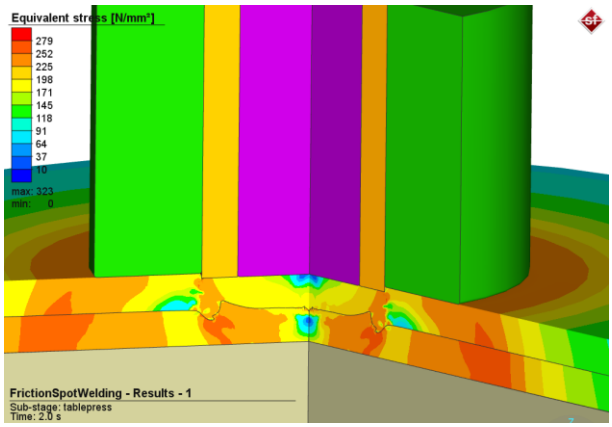

Figure 8: *Residual stresses distribution in plates*

In Figs. 9 and 10 the plastic strain in the welded joint can be observed in two moments of time, during and at the end of the welding process.

The historical graph of the plastic deformation of the upper and lower plates as well as the maximum values obtained can be seen in Fig. 11.

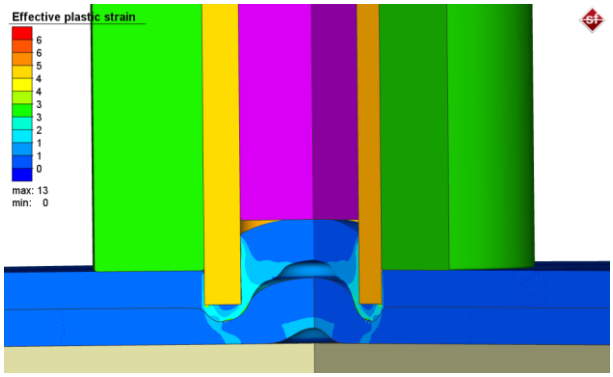

Figure 9: *Plastic strain distribution in plates at 1s*

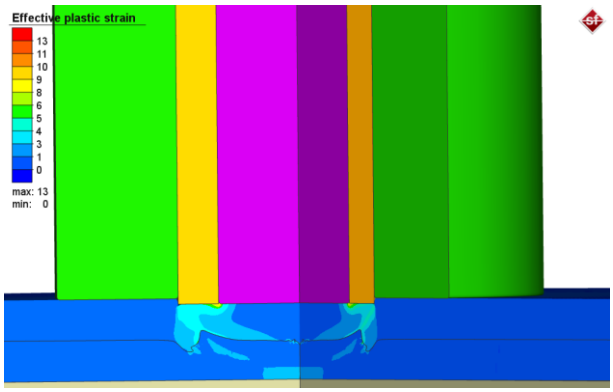

Figure 10: *Residual strain distribution in plates*

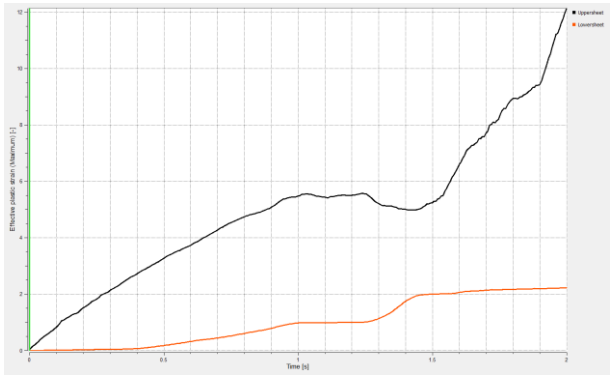

Figure 11: *Plastic strain history plot of the upper and lower plates*

5. Conclusions

The welding simulation takes into account the changes in the thermo-physical and mechanical properties of aluminum alloy 5083-O with temperature, which leads to a very accurate solution regarding the distribution and value of the thermal field and residual stress. When simulating the friction spot welding process, the consideration of the material properties as a function of temperature led to obtaining precise results. The three-dimensional analysis provides important data about the areas affected by the deformation process and the distribution of the thermal field. The maximum value of the effective stress corresponds to the area affected by deformations. The simulation results have been compared with the data available in the specialized literature and validated.

References

1. [Kubit, 2020] Kubit, A., Trzepiecinski, T., *Simulating A fully coupled thermo-mechanical numerical modelling of the refill friction stir spot welding process in Alclad 7075-T6 aluminium alloy sheets*, Archives of Civil and Mechanical Engineering, 20:117, 2020.
2. [Zou, 2021] Zou, Y., Li, W., Chu, Q., Shen, Z., Wang, F., Tang, H., Vairis, A., Liu L., *The impact of macro/microstructure features on the mechanical properties of refill friction stir spot–welded joints of AA2219 alloy with a large thickness ratio*, The International Journal of Advanced Manufacturing Technology, 2021.
3. [D'Urso, 2013] D'Urso, G., Longo M., Giardini, C., *Friction Stir Spot Welding (FSSW) of Aluminum Sheets: Experimental and Simulative Analysis*, Key Engineering Materials Vol. 549, 2013.
4. [Lage1, 2019] Lage1 and co., *A study of the parameters influencing mechanical properties and the fatigue performance of refill friction stir spot welded AlMgSc alloy*, The International Journal of Advanced Manufacturing Technology, 2019.
5. [Kubit, 2018] Kubit, A., Bucior, M., Wydrzyński, D., Trzepieciński, T., Pytel, M., *Failure mechanisms of refill friction stir spot welded 7075-T6 aluminium alloy single-lap joints*, The International Journal of Advanced Manufacturing Technology, 2018.
6. [Muci-Küchler, 2010] Muci-Küchler, H. K., Kalagara, S., Arbegast, W., *Simulation of a Refill Friction Stir Spot Welding Process Using a Fully Coupled Thermo-Mechanical FEM Model*, Journal of Manufacturing Science & Engineering - ASME, 2010.
7. [de Barros, 2017] de Barros, P.A.F., Campanelli L.C., Alcântara, N.G., dos Santos, J.F., *An investigation on friction spot welding of AA2198-T8 thin sheets*, Fat Fract Eng Mater Struc 40:535–542, 2017.
8. [Yang, 2015] Yang, H.G., Yang, H.J., Hu, X. *Simulation on the plunge stage in refill friction stir spot welding of aluminum alloys*, Proceedings of the 4th International Conference on Mechatronics Materials Chemistry and Computer Engineering, Xi'an, China, 12–13 December 2015, pp. 521–524.
9. [Cao, 2017] Cao, J.Y., Wang, M., Kong, L., Yin, Y.H., Guo, L.J., *Numerical modeling and experimental investigation of material flow in friction pot welding of Al 6061–T6*, Int J Adv Manuf Technol., 2017.
10. [D'Urso, 2016] D'Urso, G., Giardini, C., *Thermo-mechanical characterization of friction stir spot welded AA7050 sheets by means of experimental and FEM analyses*, Materials, 2016.
11. [Yang, 2018] Yang, X., Feng, W., Li, W., Xu, Y., Chu, Q., Ma, T., Wang, W., *Numerical modelling and experimental investigation of thermal and material flow in probe less friction stir spot welding process of Al 2198–T8*, Journal of Science and Technology of Welding and Joining, 2018.
12. [Zienkiewicz, 1978] Zienkiewicz, O.C., Jain, P.C., Onate, E., *Flow of Solids During Forming and Extrusion: Some Aspects of Numerical Solutions*, Int. J. Solid Struct., 1978.
13. [Sheppard, 1979] Sheppard T., Wright, D.S., *Determination of Flow Stress I-Constitutive Equation for Aluminum Alloys at Elevated Temperatures. II-Radial and Axial Temperature Distribution During Torsion Testing*, Met. Tech., 1979.